



ELSEVIER

Contents lists available at ScienceDirect

Catena

journal homepage: www.elsevier.com/locate/catena

Climate change and redoximorphosis in a soil with stagnic properties

Kristof Dorau^{a,*}, Stefan Wessel-Bothe^b, Gerhard Milbert^c, Heinz Peter Schrey^c, Dirk Elhaus^c, Tim Mansfeldt^a

^a University of Cologne, Faculty of Mathematics and Natural Sciences, Department of Geosciences, Institute of Geography, Albertus-Magnus-Platz, D-50923 Köln, Germany

^b ecoTech Umwelt-Meßsysteme GmbH, Klara-M.-Faßbinder-Straße 1A, 53121 Bonn, Germany

^c Geologischer Dienst Nordrhein-Westfalen, De-Greifff-Straße 195, 47803 Krefeld, Germany

ARTICLE INFO

Keywords:

Air-filled pore volume
Environmental monitoring
Perched water
Pedogenesis
Redoximorphic soils
Vulnerability

ABSTRACT

In soils with perched water tables, frequent changes between reducing and oxidizing conditions result in the formation of redoximorphic features (RMF). Perched water tables are linked to the presence of a low water-permeable soil horizon and high water input by precipitation. Precipitation, however, is strongly affected by climate change. Hence, we postulate that soils with a perched water table are particularly vulnerable to climate change. To verify this hypothesis, we set up a monitoring campaign from April 2014 to October 2019 at a forested Planosol in North Rhine-Westphalia, Germany. On an hourly basis, the redox potential (E_H) and air-filled pore volume (ϵ) were measured in four soil depths. Furthermore, we calculated the CWB and employed two future climate scenarios for the years 2071–2100 to discuss the consequences for RMF formation. Reducing conditions were evident in the moist hydrological winter of 2015 and 2016, while oxidizing soil conditions ($E_H > 300$ mV at pH 7) prevailed throughout the drier years (2017, 2018, 2019) for the whole soil profile. Concomitant with an increase in ϵ during spring, we observed a switch from reducing to oxidizing soil conditions at low ϵ of 0.01–0.03 cm³ cm⁻³ in the temporarily water-saturated soil horizons. At present, reducing soil conditions are limited during early spring during which manganese and iron can be mobilized from their oxides. Thus, RMF actively form but the CWB forecast until 2100 indicates a lower water input, which will diminish the period for redox-induced mineral dissolution. This study provided the essential information that soils with a perched water table are specifically vulnerable under progressing climate change. Presumably, RMF become more and more relictic that needs to be validated in the future.

1. Introduction

Redoximorphic features (RMF) in soils are the result of frequent changes between reduction and oxidation (redox) (Reddy and DeLaune, 2008). When the oxygen (O_2) pool of a soil is exhausted during prolonged periods of water saturation, microorganisms utilize electron acceptors other than O_2 in a stepwise manner and reduce them to their soluble and mobile counterparts (e.g., tetravalent manganese (Mn^{IV}) to Mn^{2+} ; trivalent iron (Fe^{III}) to Fe^{2+}) (Gotoh and Patrick, 1972; Gotoh and Patrick, 1974). After re-aeration, the mobile metal species are immobilized by oxidation as their corresponding oxides. The redistribution and accumulation of Mn and Fe oxides forms RMF under variable redox conditions and is an important soil forming process used in many soil classifications (AG Boden, 2005; IUSS Working Group WRB, 2015; Soil Survey Staff, 2014) and nowadays known as redoximorphosis (Scheffer and Schachtschabel, 2018). Prolonged periods of water saturation by groundwater favors the development of gleyic

properties (in Gleysols), and periods of temporarily perched water favors stagnic properties (in Planosols, Plinthosols and Stagnosols) (IUSS Working Group WRB, 2015). Perched water is also known as ‘episaturation’ (Soil Survey Staff, 2014), ‘surface water’ (IUSS Working Group WRB, 2015), or ‘Stauwasser’ (AG Boden, 2005) but termed to variable extent throughout the literature (e.g., ‘surface water soils’ (Blume and Schlichting, 1985); ‘seasonally waterlogged soils’ (Cornu et al., 2009); ‘perched seasonal water table’ (Owens et al., 2001)). An upper reduced soil horizon with bleached colors combined with a lower oxidized horizon with browner colors exemplify stagnic properties (Chesworth, 2008) that can be identified due to characteristic oximorphic and reductimorphic colors (IUSS Working Group WRB, 2015).

The particle size distribution controls the water permeability of soils and is a key component of soils having a perched water table. Two characteristic features can be differentiated for soils with a perched water table: (i) a pre-dominant fine sandy-silty matrix with high field-capacity and (ii) a coarser textured substrate underlain by a clay-rich

* Corresponding author.

E-mail address: k.dorau@uni-koeln.de (K. Dorau).

<https://doi.org/10.1016/j.catena.2020.104528>

Received 13 November 2019; Received in revised form 11 February 2020; Accepted 18 February 2020

0341-8162/ © 2020 Elsevier B.V. All rights reserved.

subsoil horizon of low water-permeability (Blume and Schlichting, 1985). These genetic differences are incorporated within the German soil classification exemplified by soil types such as ‘Haftpseudogley’ for the former and ‘Pseudogley’ or ‘Stagnogley’ for the latter textural feature having RMF (AG Boden, 2005). Besides interflow, in most cases soils with perched water table receive their water intake solely by precipitation and typically demonstrate reducing conditions only seasonally because of precipitation distribution. Hence, we postulate that these soils are vulnerable to changes in the climatic conditions and the current redox status under global warming along with modifications in precipitation dynamics do not necessarily reflect persistent RMF that formed under different climatic conditions in the past. The persistence of RMF renders it particularly difficult to distinguish between relict or recent redoximorphosis. Overall, redox dynamics in soils with perched water table are highly variable both spatially and temporally because of soil properties and precipitation dynamics.

A key parameter to characterize and quantify the soil redox milieu is the redox potential (E_H) in units of electrochemical energy (DeLaune and Reddy, 2005). Although E_H has only a semi-quantitative significance in soils, due to soil complexity and thermodynamic limitations on the use of Pt electrodes (Bohn, 1971; Whitfield, 1974), numerous publications have demonstrated the linkage of E_H to abiotic processes such as aeration or water table fluctuations (Glinski and Stepniewski, 1985; Mansfeldt, 2003). Fortunately, the Pt electrode responds to changes in the electroactive $Fe^{2+} - Fe^{3+}$ redox pair and, thus, the E_H is supportive to detect the occurrence of dissolved and adsorbed Fe^{2+} under field conditions (Cogger et al., 1992; Mansfeldt, 2004). Indeed, the IUSS Working Group proposed an E_H drop below 177 mV at pH 7 (equals a rH of 20; IUSS Working Group WRB, 2015) for indicating of Fe reducing conditions, a prerequisite to actively form RMF. In addition to Fe, $Mn^{2+} - Mn^{3+/4+}$ participates in electron transfer reactions and is likewise an important constituent to form RMF. Another important soil parameter that is easy to measure is the soil water content and related to it the air-filled pore volume (ϵ). Considering the relation between E_H and ϵ , an increase in ϵ decreases the volume of anaerobic soil and facilitates oxidizing soil conditions over time. Previous studies have already pointed out this relation (Flühler et al., 1976; Glinski and Stepniewski, 1985; Grable and Siemer, 1968) that has been quantitatively assessed within undisturbed soil cores by Dorau et al. recently (2018).

To investigate the interactive dependency between atmospheric, soil hydrologic and redox conditions, we set-up an E_H monitoring campaign in a forested soil located in the temperate region. The objectives of this study were to (i) assess and quantify the E_H - ϵ relation in a forested Planosol under the present climatic conditions, and (ii) discuss the driving forces of soil formation under perched water table conditions in light of two future climatic scenarios. For this reason, the climatic water balance (CWB) was calculated for the current E_H and ϵ monitoring campaign (April 2014 to October 2019) to evaluate the site-specific impacts of meteorological forcing on redox dynamics. In addition, the CWB was calculated for the reference period from 2071 to 2100 to assess the propensity for the development of redoximorphic features in the future, i.e., under climate change.

2. Materials and methods

2.1. Study site

The study site was in Kottenforst Forest in southern North Rhine-Westphalia close to the city of Bonn (50° 40' 18" N, 7° 02' 48" E; 168 m asl). The subsoil features colluvic Pleistocene material overlain by clay and silt-rich aeolian Weichsel sediments. The reference soil group is Epidystric Albic Planosol (Ferric) (IUSS Working Group WRB, 2015) and covers 80–90% of the study site. According to the German classification system (AG Boden, 2005), the soil is a Parabraunerde-Pseudogley and approximates the great groups of Albaqualls,

Albaqualls and Argialbolls (Soil Survey Staff, 2014). The site is covered with common oak (*Quercus pedunculata*) and hornbeam (*Carpinus betulus*) with minor contribution of small-leaved lime (*Tilia cordata*). The mean annual air temperature is 10.8 °C with on average of 630 mm of precipitation (reference period 1981–2010). Interflow is of minor importance at the study site because the slope of the terrain is < 1°.

2.2. Soil properties

The morphology of the soil profile was described after excavating a pit that was located 5 m from the monitoring plot where data was collected. Disturbed soil samples were taken according to the installation depths of the soil probes. The samples were oven-dried at 40 °C and sieved (< 2 mm) to measure the soil pH potentiometrically in deionized H₂O mixed 5:1 with soil (v/v) and the particle-size distribution after pre-treatment with H₂O₂ by the sieve and settling method. Subsamples were pulverized in a mixer mill (MM400, Retsch, Haan, Germany) to determine organic carbon (OC) and nitrogen (N) by dry combustion with a CNS analyzer (vario EL cube, Elementar, Hanau, Germany). The oxidic Mn and Fe oxide pool was extracted by using oxalate (Schwertmann, 1964) and dithionite-citrate-bicarbonate solution (DCB; Mehra and Jackson, 1960) following analysis of Mn and Fe concentrations by ICP-OES (SPECTROGREEN, Spectro, Kleve, Germany). Concomitantly, undisturbed soil samples were taken by steel cylinders (250 cm³) to determine the water retention curve and to derive soil hydraulic properties with quintuplicate repetition (Schindler et al., 2010; UMS, 2015). The saturated hydraulic conductivity was measured by the falling head method with eightfold repetition (KSAT®, UMS, Munich, Germany). The bulk density was determined at the same steel cylinder used to determine soil hydraulic properties and saturated conductivity by weighting after oven-heating for 24 h at 105 °C.

2.3. Field monitoring

The monitoring plot was 3 by 3 m and equipped with the following instruments in the Eg (25 cm), Btg (65 and 90 cm), and 2Bg (120 cm) horizons in March 2014: E_H measurements were conducted with permanently-installed Pt electrodes in threefold repetitions placed in stellar constellation around a silver-silver chloride reference electrode (ecoTech, Bonn, Germany; 3 M KCl internal electrolyte). The readings were converted to the standard hydrogen electrode by adding 207 mV to calculate the E_H . Readings were adjusted to pH 7 by using Eq. (1) and by considering the pH of field-collected soil samples as commonly done for comparability (Bohn, 1971):

$$E_H(\text{pH } 7) = E_H - (\text{pH} - 7) \cdot 59 \text{ mV.} \quad (1)$$

To obtain matric potentials, Tensiomark sensors (ecoTech, Bonn, Germany) were installed in duplicate in close vicinity (~10 cm horizontal distance) to the Pt electrodes at the corresponding depths. We used the Durner equation based on a van Genuchten-Mualem-type function to convert matric potential data into volumetric water contents (Durner, 1994). The soil hydraulic properties were derived from steel cylinder sampling. In order to calculate ϵ , we subtracted the soil water content at saturation (θ_s ; cm³ cm⁻³) by the converted soil water content determined in the field (θ ; cm³ cm⁻³). All readings were measured on hourly basis, stored in a data logger (enviLog Maxi, ecoTech, Bonn, Germany) and sent by GPRS.

2.4. Statistical analysis

We analyzed the dataset by a holistic and universal statistical approach in order to derive a quantitative relation between E_H and ϵ and investigate critical ϵ thresholds (ϵ_{th}) that facilitate the switch from reducing towards oxidizing soil conditions. Therefore, we followed the procedure presented by Nakamura et al. (2018). Very briefly, the dichotomy of the E_H and ϵ data was assumed with an E_H reference

level > 300 mV at pH 7 (E_{Href} ; ‘threshold’ between reducing and oxidizing soil conditions) and with arbitrarily specified values of ε_0 with an increment $\Delta\varepsilon_0$ of $0.01 \text{ cm}^3 \text{ cm}^{-3}$. The E_H threshold was proposed by Reddy and DeLaune (2008) and is slightly higher than the value of 177 mV according to the IUSS Working Group WRB (2015) to characterize reducing conditions. While the former value integrates the important range of Mn oxide reduction between 200 and 300 mV at pH 7 (Dorau and Mansfeldt, 2015; Gotoh and Patrick, 1972), the latter classification scheme ignores the $\text{Mn}^{2+} - \text{MnO}_2$ redox system and the formation of Mn concretions and nodules over time. Therefore, we consider the value of 300 mV more appropriate for our objectives. After defining E_{Href} and specifying $\Delta\varepsilon_0$, the dataset was divided into four groups: $n1$ ($\varepsilon_{th} < \varepsilon_0$ and $E_H > E_{Href}$), $n2$ ($\varepsilon_{th} < \varepsilon_0$ and $E_H < E_{Href}$), $n3$ ($\varepsilon_{th} > \varepsilon_0$ and $E_H > E_{Href}$), and $n4$ ($\varepsilon_{th} > \varepsilon_0$ and $E_H < E_{Href}$). Consecutive computations were made for ε_0 (e.g., from water saturation towards an ε of $0.20 \text{ cm}^3 \text{ cm}^{-3}$), and the valid numbers of each group were counted for which the prerequisites were met. The counted numbers were implemented into the function $f(\varepsilon_0) = n1 \cdot n4 - n2 \cdot n3$ and ε_{th} was identified by seeking for ε_0 with the maximum value of f (ε_0). For further statistical analyses of the CWB, E_H , and ε , we tested for normality by the Shapiro-Wilk test, and because of non-normally distributed data, the Spearman’s rank correlation coefficient was calculated by XLSTAT-Pro software (Addinsoft V.2014.1.05.). If not otherwise specified, the data are presented as mean with the standard error of the mean (\pm).

2.5. Climatic water balance and future scenarios

We obtained meteorological data from the synoptic weather station Euskirchen (18 km west of the site; German Meteorological Service, 2009), to calculate the monthly CWB defined as the difference between evapotranspiration and precipitation. The advantage to implement the nearby weather station is that we can access a coherent dataset that is present for three fundamental periods incorporated in this study, which is the reference period from 1981 to 2010, the ambient monitoring period from 2014 to 2019, and two future scenarios from 2071 to 2100. The data enabled to calculate rates of evapotranspiration in mm d^{-1} by the Haude formula with

$$PET_{Haude} = f \cdot e_s \left(1 - \frac{F}{100} \right). \quad (2)$$

The plant-specific coefficient f refers to individual beech trees for each month and approximates the conditions found at the study site

Table 1

Soil properties of the Planosol monitoring depths (shown are mean \pm standard error).

		25	65 + 90	120
Horizon	(-)	Eg	Btg	2Bg
Matrix	(-)	10YR 6/3	10YR 4/6	7.5YR 5/3
Reductomorphic	(-)	-	10YR 6/3 20%	7.5YR 6/2 20%
Oximorphic	(-)	7.5YR 5/8 1%	10YR 5/8 30%	7.5YR 5/8 30%
pH in H ₂ O	(-)	4.5 \pm 0.1	4.9 \pm 0.1	5.1 \pm 0.1
Oxalate extractable Mn	/ g kg ⁻¹	0.38 \pm 0.03	0.15 \pm 0.08	0.05 \pm 0.01
Oxalate extractable Fe (Fe _o)	/ g kg ⁻¹	1.97 \pm 0.01	2.77 \pm 0.19	2.63 \pm 0.42
Dithionite extractable Fe (Fe _{DCE})	/ g kg ⁻¹	5.91 \pm 0.03	9.84 \pm 0.12	11.40 \pm 0.57
Fe _o /Fe _{DCE}	(-)	0.33	0.28	0.23
Organic carbon (OC)	/ g kg ⁻¹	3.8 \pm 0.2	2.2 \pm 0.1	1.8 \pm 0.1
Nitrogen (N)	/ g kg ⁻¹	0.3 \pm 0.04	0.3 \pm 0.02	0.2 \pm 0.01
OC/N	(-)	12.7	7.3	9
Sand	/ g kg ⁻¹	68 \pm 5	50 \pm 7	148 \pm 22
Silt	/ g kg ⁻¹	809 \pm 30	675 \pm 21	570 \pm 28
Clay	/ g kg ⁻¹	122 \pm 15	276 \pm 22	283 \pm 11
Porosity	/ cm ³ cm ⁻³	0.43 \pm 1.2	0.43 \pm 0.6	0.39 \pm 2.3
Air capacity (θ at pF 1.8)	/ cm ³ cm ⁻³	0.07 \pm 1.3	0.05 \pm 0.6	0.04 \pm 0.4
Permanent wilting point (θ at pF 4.2)	/ cm ³ cm ⁻³	0.08 \pm 0.2	0.20 \pm 0.2	0.21 \pm 0.8
Bulk density	/ g cm ⁻³	1.51 \pm 0.1	1.55 \pm 0.1	1.65 \pm 0.1
Saturated hydraulic conductivity	/ cm d ⁻¹	21.0 \pm 20	2.0 \pm 0.7	3.4 \pm 4.3

(Haude, 1952), F is the relative humidity (%), and e_s is the water vapor saturation deficit (hPa) for air, which was calculated by entering the air temperature at 14:00 CET into the formula

$$e_s = 6.11 \cdot e^{\frac{(17.62 \cdot T)}{(243.12 + T)}}. \quad (3)$$

The future scenarios are based on the regional climate model STAR (German Meteorological Service, 2009; Orłowsky et al., 2008; Potsdam Institute for Climate Impact Research, 2013) and account for the Representative Concentration Pathways (RCPs), 2.6 and 8.5, that reflect the possible range of radiative forcing with 2.6 and 8.5 W m^{-2} proposed by the Intergovernmental Panel on Climate Change.

3. Results and discussion

3.1. Soil properties

Soils influenced by perched water tables (i) contain *stagnic properties* and (ii) *reducing conditions* must temporarily prevail (IUSS Working Group WRB, 2015). These prerequisites are fulfilled as indicated by oximorphic and reductomorphic color pattern covering $\geq 50\%$ area within the upper 50 cm (Table 1 and Fig. 1), and reducing conditions with $E_H < 300$ mV at pH 7 persist for some time during the year (Fig. 2b and d). If an abrupt textural change occurs the soil is a Planosol, which is the case here (IUSS Working Group WRB, 2015). The pH slightly increased from the Eg horizon with pH 4.5 towards pH 5.1 in the subsoil (Table 1). The OC content ranged between 3.8 and 1.8 g kg^{-1} , with narrow C/N ratios. Sand contents were generally low while silt contents were high due to the aeolian-deposited sediments. The occurrence of perched water is strongly bound to the hydraulic conductivity of a soil which, in turn, is negatively correlated with the clay content (Tsubo et al., 2007). Hydraulic conductivities are seldom measured to relate redox dynamics under perched water table conditions (Hseu and Chen, 1996; Megonigal et al., 1993; Owens et al., 2001) but are mainly responsible, together with climatic conditions, for the degree of bleaching within the Eg horizon (Blume and Schlichting, 1985). The saturated hydraulic conductivity of 2.0 ± 0.7 and $3.4 \pm 4.3 \text{ cm d}^{-1}$ in the dense Btg and 2Bg horizon is similar to other studies, e.g. with 1.8 cm d^{-1} (Garg et al., 2005) or 1.7 cm d^{-1} (Hseu and Chen, 1996).

3.2. CWB, ε , and E_H interactions

The CWB ranged between -178 mm during the dry hydrological

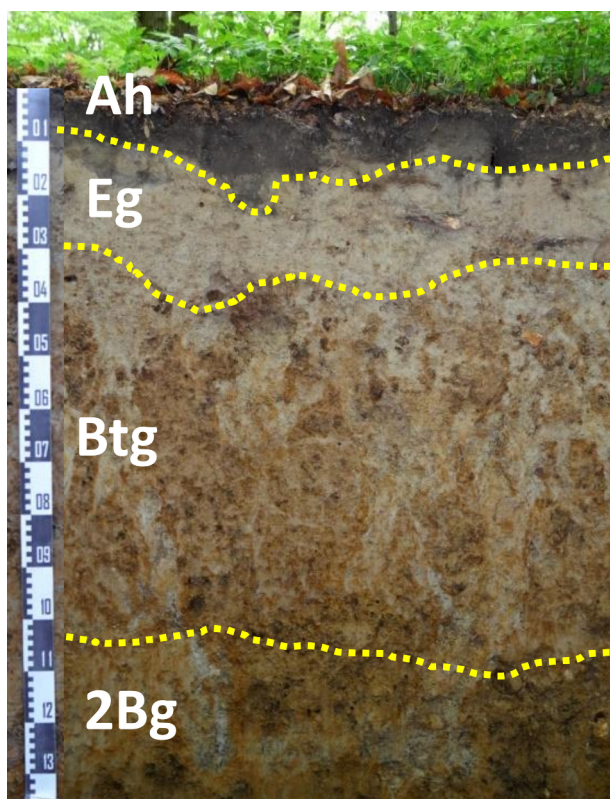


Fig. 1. Image of the Epidystric Albic Planosol (Ferric) at Kottenforst Forest near Bonn, North Rhine-Westphalia, Germany. The monitoring depths were at 25, 65, 90, and 120 cm depths for redox potential and matric potential readings. The soil is a Parabraunerde-Pseudogley (Sw-Ah/Sw-Al/Sw/Sd/IISd) according to the German soil classification (A color version of this image is available in the online version).

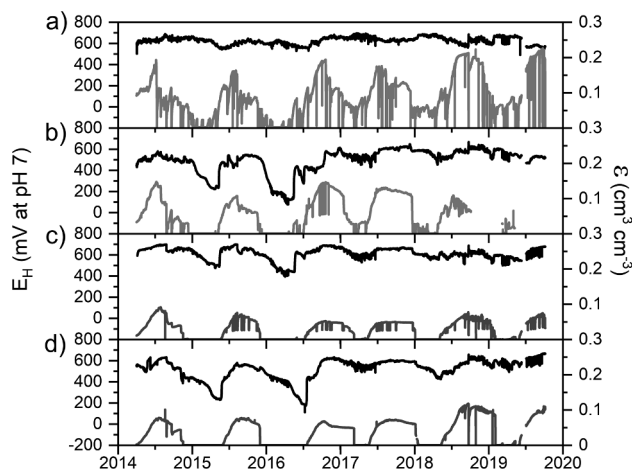


Fig. 2. Development of the mean redox potential (E_H ; black line) and air-filled pore volumes (ϵ ; grey line) at 25 (a), 65 (b), 90 (c), and 120 cm (d) soil depths on an hourly basis for the monitoring period from April 2014 to October 2019.

summer of 2018 and 406 mm during the moist hydrological winter in 2015 (Table 2). Typical for mid-latitude regions, the CWB was lower during the hydrologic summer (high evapotranspiration) compared with the hydrologic winter (low evapotranspiration). The relation between the CWB and ϵ is negatively correlated (Table 3) with the following specific features: (i) ϵ declined towards the hydrologic winter and peaked during the hydrologic summer (Fig. 2a to d), (ii) ϵ declined with soil depth in each year, since water consumption by

evapotranspiration in the well-rooted topsoil was higher than in the subsoil (Table 2), (iii) the period with $\epsilon > 0.001 \text{ cm}^3 \text{ cm}^{-3}$ (i.e. pores were not water-saturated) declined with soil depth for the entire period (Fig. 2a to d), and (iv) differences in the individual hydrologic years have major impacts with respect to ϵ (Table 2). Values of ϵ peaked in the summer, up to $0.25 \text{ cm}^3 \text{ cm}^{-3}$, and were close to water saturation during the hydrologic winters, especially in 2015 and 2016 (Fig. 2).

Considering the redox dynamics, oxidizing soil conditions prevailed constantly at 25 and 90 cm depths (Fig. 2a and c), but the soil was reduced ($E_H < 300 \text{ mV}$) for 14% and 7% of the time at 65 and 120 cm depths, respectively (Fig. 2b and d). A seasonal E_H oscillation was evident within these depths, with an E_H decline during the hydrologic winters of 2015 and 2016 followed by a sharp E_H increase from March to May. The relation between E_H and ϵ was significantly positive correlated and increased with depth as indicated by Spearman's rank correlations (Fig. 2b–d, Table 3).

The ϵ threshold values that separate the data into oxidizing and reducing soil conditions revealed a relatively small ϵ of 0.03 and $0.01 \text{ cm}^3 \text{ cm}^{-3}$ at 65 and 120 cm depths, respectively (Fig. 3). These thresholds, which were derived by the dichotomy of the dataset, were lower than the ones reported in a laboratory-based study that ranged between 0.036 ± 0.006 to $0.047 \pm 0.005 \text{ cm}^3 \text{ cm}^{-3}$ for a sandy soil and 0.048 ± 0.008 to $0.085 \pm 0.007 \text{ cm}^3 \text{ cm}^{-3}$ for a silt loam (Dorau et al., 2018). Modifications of the measurement principle results in variable sensor accuracy and might explain this finding with heat dissipation matric potential sensors ($\pm 30 \text{ hPa}$) in this study compared with tensiometric readings ($\pm 1.5 \text{ hPa}$) for the laboratory study (Dorau et al., 2018). Independent of this, the dichotomous separation of the E_H - ϵ data set is useful for parametrizing study sites and predicting changes in redox dynamics, e.g., when soil water content is measured, but E_H data is missing. The advantages of this statistical approach to derive the E_H - ϵ relation comprise an independent, universal procedure usable by stakeholders and practitioners dealing with ecological functions and geochemical cycling.

3.3. Future prospects of redox dynamics in Kottenforst Forest

Factors that are conducive for the development of reducing conditions and the formation of RMF include (i) water saturation of the soil, (ii) adequate OC and (iii) elevated soil temperatures for sufficient microbial activity as well as (iv) adequate supplies of Fe and Mn (summarized by D'Amore et al., 2004). This generalized view is very site-specific and it is now recognized, for instance, that the occurrence of RMF in soils is more related to the lengths of time the soil is in a reduced state than it is in a water saturated state (Vepraskas, 2015; Vepraskas and Wilding, 1983). This is exemplified at Kottenforst Forest in the following: the E_H was consecutively at oxidizing soil conditions from 2017 to 2019, even though water was perched in 65, 90, and 120 cm depth during that period (Fig. 4b). The relatively moist years in 2015 and 2016 with $\epsilon < 0.03 \text{ cm}^3 \text{ cm}^{-3}$ in the topsoil, however, stimulated the onset of reducing soil conditions in the subsoil (Fig. 4c) due to impaired O_2 diffusion from the atmosphere. This reflects the decoupled behavior that water saturation does not necessarily foster the prevalence of reducing soil conditions.

Under the ambient climatic conditions, reducing conditions occurred in two out of five years. Both RCP scenarios from 2071 to 2100 indicate that the study site will become drier, specifically during the hydrologic summer in comparison with the reference period from 1981 to 2010 (Table 2). The dry hydrologic summer of 2018 with a CWB of -187 mm (Table 2) can be seen as a harbinger of what we have to expect. Since the CWB was negatively correlated with ϵ in the upper soil horizons and ϵ , in turn, affected the prevalence of reducing soil conditions, the likelihood for the occurrence of annual reducing conditions at this study site is negligible in the future. In addition, presumable changes in the distribution of precipitation will enhance the likelihood for this scenario. Recent observations highlight a trend towards high

Table 2

Meteorological and soil hydrological data for the reference period from 1981 to 2010, the hydrological years 2014 to 2019, and two future scenarios from 2071 to 2100 (each year refers to the period from 1st of November to 31st of October).

		Precipitation/mm	Sum of precipitation/mm	CWB ^c /mm	CWB/mm	$\epsilon^d/\text{cm}^3 \text{cm}^{-3}$			
						25	65	90	120
Ref	HW ^a	269	632	166	207	n.d.			
	HS ^b	363		41					
2014	HW	n.d. ^c	n.d.	n.d.	n.d.	n.d.			
	HS	566		291					
2015	HW	434	934	406	491	0.032 ± 0.004	0.007 ± 0.001	0.002 ± 0.001	0.002 ± 0.002
	HS	500		85		0.103 ± 0.005	0.069 ± 0.006	0.043 ± 0.011	0.049 ± 0.009
2016	HW	426	864	399	478	0.029 ± 0.006	0.008 ± 0.001	0.006 ± 0.002	0.010 ± 0.001
	HS	438		79		0.115 ± 0.008	0.072 ± 0.020	0.022 ± 0.008	0.027 ± 0.002
2017	HW	277	680	253	336	0.086 ± 0.004	0.070 ± 0.016	0.027 ± 0.012	0.036 ± 0.001
	HS	403		83		0.140 ± 0.007	0.106 ± 0.026	0.038 ± 0.009	0.053 ± 0.006
2018	HW	346	629	318	140	0.074 ± 0.004	0.039 ± 0.009	0.017 ± 0.003	0.025 ± 0.003
	HS	283		-178		0.194 ± 0.013	0.074 ± 0.037	0.046 ± 0.009	0.070 ± 0.011
2019	HW	345	509	314	186	0.096 ± 0.009	0.058 ± 0.012	0.021 ± 0.005	0.047 ± 0.003
	HS	164		-128		0.100 ± 0.013	0.002 ± 0.009	0.014 ± 0.003	0.018 ± 0.008
RCP2.6 ^f	HW	265	591	143	137	n.d.			
	HS	326		-6					
RCP8.5 ^f	HW	282	593	124	9	n.d.			
	HS	311		-114					

^a Hydrological winter (period from November 1 to April 30).

^b Hydrological summer (period from May 1 to October 31).

^c Climatic water balance.

^d Air-filled pore volume.

^e Not determined.

^f Representative Concentration Pathways with a radiative forcing of 2.6 and 8.5 W m⁻².

Table 3

Spearman's rank correlation coefficient for selected variables on monthly basis of the Planosol monitoring depths ($n = 132$).

Depth cm	E_H vs. ϵ^a	CWB ^b vs. ϵ	CWB vs. E_H
25	-0.038	-0.621***	0.248
65	0.531***	-0.501***	-0.0347
90	0.741***	-0.240	-0.157
120	0.767***	-0.114	0.131

*** Significant at $P < 0.001$

^a Air-filled pore volume.

^b Climatic water balance.

precipitation and convective weather conditions in Central Europe (Bárdossy and Caspary, 1990; Hoy et al., 2014) with the probability for more intense precipitation events over most mid-latitude land masses in the future (IPCC, 2014). This has implications for the redox dynamics of soils with perched water table because (i) short-lasting convective precipitation (high intensity) will result in surface run-off depending on the relief in comparison with long-lasting advective precipitation (low intensity) and (ii) enhanced evapotranspiration will diminish the wet period and therefore the extent of reducing soil conditions. Thus, there is a curtailed period for RMF to form. Soils having a perched water table receive their water intake exclusively by precipitation and, thus, are particularly vulnerable to changes in the dynamics of precipitation. Additional external factors (e.g., weather/climate, soil temperature; Fig. 5a) along with internal factors (e.g., pH, organic matter, parent material, Mn and Fe oxide characteristics; Fig. 5b) control the distribution of RMF in soils with perched water table in space and time. These factors cannot be portrayed individually and, thus, climate change induced impacts on biogeochemical cycles in the future are particularly site-specific. To distinguish whether RMF are relictic or redoximorphosis is still active it is possible to use (i) dyes that react with Fe^{2+} to colored compounds (Childs, 1981), (ii) conduct soil solution sampling following the terminal electron-accepting processes (TEAPs) approach (Chapelle et al., 1995), and (iii) employ Indicator of

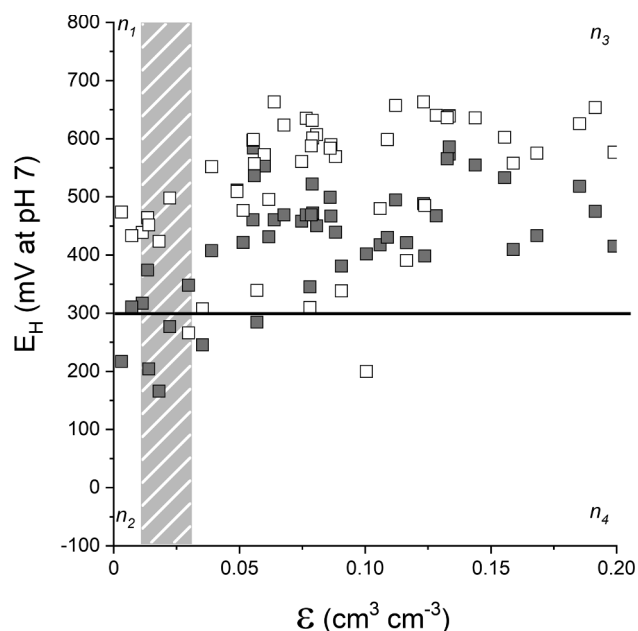


Fig. 3. Dichotomy diagram of data at 65 (dark grey) and 120 cm (white) soil depths with respect to air-filled pore volumes (ϵ) and redox potentials (E_H). The increments for ϵ was arbitrarily set to 0.01 $\text{cm}^3 \text{cm}^{-3}$ and the reference threshold for E_H was set to 300 mV (threshold between oxidizing and reducing soil conditions). The dataset was divided into four groups of n_1 , n_2 , n_3 , and n_4 (for a detailed description see above).

Reduction in Soils (IRIS) tubes coated with synthetic $\text{Mn}^{\text{III,IV}}$ (Dorau and Mansfeldt, 2015) or Fe^{III} oxide (Jenkinson and Franzmeier, 2006; Rabenhorst and Burch, 2006). Each method has its advantages and shortcomings but long-term trends of reducing conditions in soils are studied at best by permanent installed Pt electrodes with recording of the E_H (Dorau and Mansfeldt, 2016; Mansfeldt, 2020). It is highly

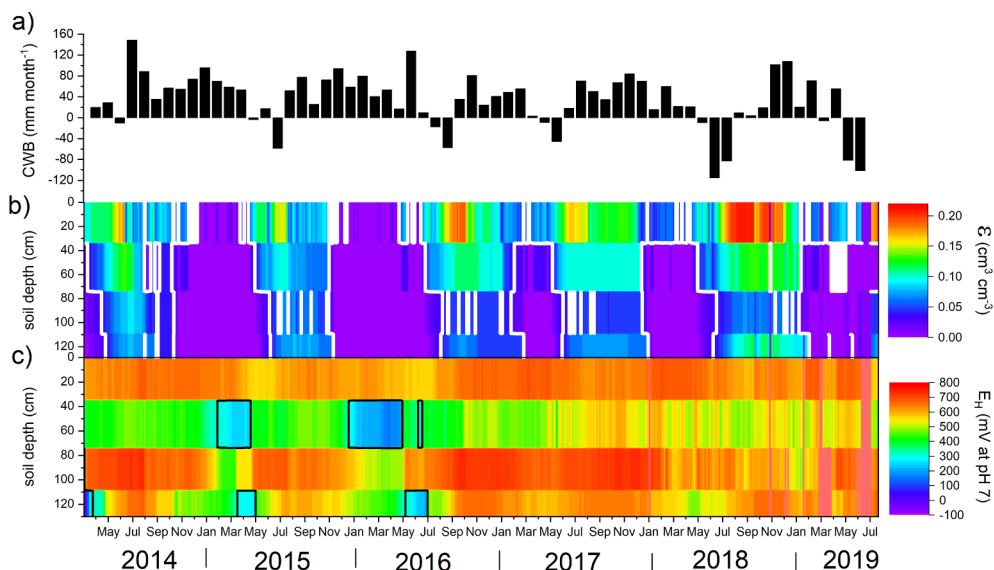


Fig. 4. Development of the climatic water balance on monthly basis (CWB; a) and contour plots of the air-filled pore volume (ϵ ; b) and the redox potential (E_H ; c) on hourly basis for the monitoring period from April 2014 to October 2019. The temporal and spatial extent where ϵ is $< 0.03 \text{ cm}^3 \text{ cm}^{-3}$ is highlighted by white contour lines (b) and the period where E_H is $< 300 \text{ mV}$ at pH 7 by black contour lines (c). The data contain individual redox electrode readings for E_H with averaged ϵ data from matric potential readings in duplicate (A color version of this image is available in the online version).

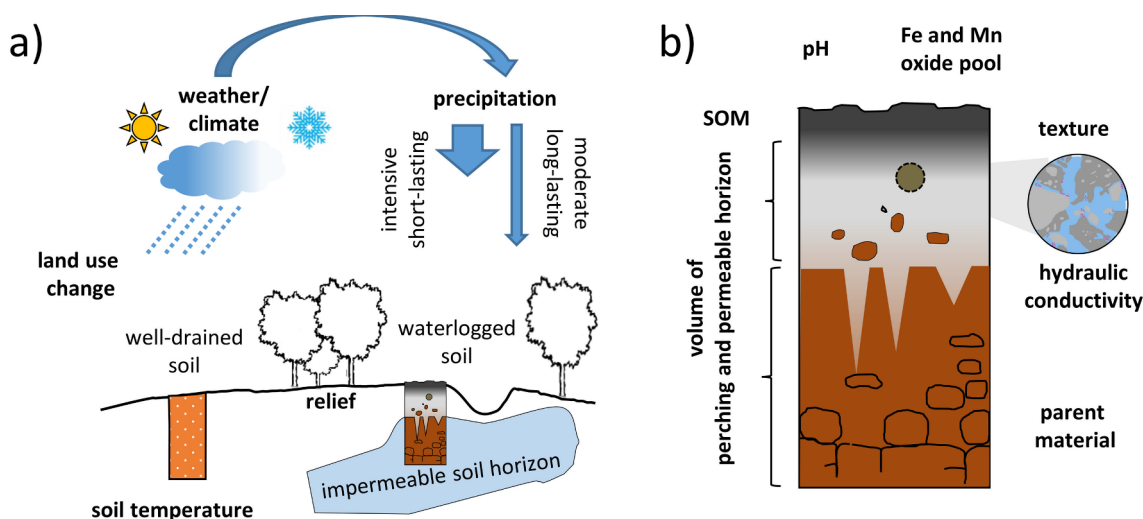


Fig. 5. Sketch of external (a) and internal (b) factors that contribute to the formation of soils with a perched water table (A color version of this image is available in the online version).

recommended to assess the climate change induced risks for soils by empirical data as exemplified within this study contrary over a qualitative manner or by mathematical simulations as commonly performed in soil sciences (Pfeiffer et al., 2017).

4. Conclusions

This study provided important information on the E_H - ϵ interaction under *in situ* conditions at a forested Planosol. The switch from reducing towards oxidizing soil conditions in temporarily water-saturated soil horizons occurred at low ϵ of 0.01 and 0.03 $\text{cm}^3 \text{ cm}^{-3}$. Reducing conditions were evident under perched water table conditions in 2015 and 2016 but absent from 2017 to 2019. From a thermodynamic point of view, it is realistic that Mn and Fe oxides form actively RMF but shifts in the CWB are likely responsible that reducing conditions will diminish in the future and RMF are relictic. Hence, soils with stagnic properties are very vulnerable under the aspect of climate change. We encourage implementing causal relations in order to obtain site-specific behaviors for redox dynamics, such as the E_H - ϵ -CWB feedback. This creates knowledge-based possibilities for stakeholders to determine the behavior of redoximorphic processes in soils featuring a perched water table.

Declaration of Competing Interest

The authors declare that they have no known competing financial interests or personal relationships that could have appeared to influence the work reported in this paper.

Acknowledgements

We greatly acknowledge the support by Mrs. Ylva Hauf from the Potsdam Institute for Climate Impact Research. Mr. Rainer Janßen from the Geological Survey North Rhine-Westphalia was a great support during the fieldwork. This research did not receive any specific grant from funding agencies in the public, commercial, or not-for-profit sectors.

References

AG Boden, 2005. *Bodenkundliche Kartieranleitung*, 5th ed. Schweizerbart science publishers, Stuttgart, Germany.
 Bárdossy, A., Caspary, H.J., 1990. Detection of climate change in Europe by analyzing European atmospheric circulation patterns from 1881 to 1989. *Theor. Appl. Climatol.* 42, 155–167.
 Blume, H.-P., Schlichting, E., 1985. Morphology of wetland soils. In: Anonymous (Ed.),

- Wetland Soils: Characterization, Classification and Utilization. International Rice Research Institute Los Banos, Philippines, pp. 161–176.
- Bohn, H.L., 1971. Redox potentials. *Soil Sci.* 112, 39–45.
- Chapelle, F.H., McMahon, P.B., Dubrovsky, N.M., Fujii, R.F., Oaksford, E.T., Vroblesky, D.A., 1995. Deducing the distribution of terminal electron-accepting processes in hydrologically diverse groundwater systems. *Water Resour. Res.* 31, 359–371.
- Chesworth, W., 2008. *Encyclopedia of Soil Science*. Springer, Dordrecht, The Netherlands.
- Childs, C.W., 1981. Field-tests for ferrous iron and ferric-organic complexes (on exchange sites or in water soluble forms) in soils. *Aust. J. Soil Res.* 19, 175–180.
- Cogger, C.G., Kennedy, P.E., Carlson, D., 1992. Seasonally saturated soils in the Puget lowland II. measuring and interpreting redox potentials. *Soil Sci.* 154, 50–58.
- Cornu, S., et al., 2009. Impact of redox cycles on manganese, iron, cobalt, and lead in nodules. *Soil Sci. Soc. Am. J.* 73, 1231–1241.
- D'Amore, D.V., Stewart, S.R., Huddleston, J.H., 2004. Saturation, reduction, and the formation of iron–manganese concretions in the Jackson-Prairie Wetland. *Oregon. Soil Sci. Soc. Am. J.* 68, 1012–1022.
- DeLaune, R.D., Reddy, K.R., 2005. Redox potential. In: Hillel, D. (Ed.), *Encyclopedia of Soils in the Environment*. Academic Press, San Diego, CA, USA, pp. 366–371.
- Dorau, K., Mansfeldt, T., 2015. Manganese-oxide-coated redox bars as an indicator of reducing conditions in soils. *J. Environ. Qual.* 44, 696–703.
- Dorau, K., Mansfeldt, T., 2016. Comparison of redox potential dynamics in a diked marsh soil: 1990 to 1993 versus 2011 to 2014. *J. Plant Nutr. Soil Sci.* 179, 641–651.
- Dorau, K., Luster, J., Mansfeldt, T., 2018. Soil aeration: the relation between air-filled pore volume and redox potential. *Eur. J. Soil Sci.* 69, 1035–1043.
- Durner, W., 1994. Hydraulic conductivity estimation for soils with heterogeneous pore structure. *Water Resour. Res.* 30, 211–223.
- Flühler, H., Stolzy, L.H., Ardakani, M.S., 1976. A statistical approach to define soil aeration in respect to denitrification. *Soil Sci.* 122, 115–123.
- Garg, K.K., Jha, M.K., Kar, S., 2005. Field investigation of water movement and nitrate transport under perched water table conditions. *Biosyst. Eng.* 92, 69–84.
- German Meteorological Service, 2009. *Daten der Klimastationen des Deutschen Wetterdienstes, Offenbach, Germany*.
- Glinski, J., Stepniowski, W., 1985. *Soil Aeration and Its Role for Plants*. CRC Press, Boca Raton, FL, USA.
- Gotoh, S., Patrick, W.H., 1972. Transformation of manganese in a waterlogged soil as affected by redox potential and pH. *Soil Sci. Soc. Am. Proc.* 36, 738–742.
- Gotoh, S., Patrick, W.H., 1974. Transformation of iron in a waterlogged soil as influenced by redox potential and pH. *Soil Sci. Soc. Am. Proc.* 38, 66–71.
- Grable, A.R., Siemer, E.G., 1968. Effects of bulk density, aggregate size, and soil water suction on oxygen diffusion, redox potentials, and elongation of corn roots. *Soil Sci. Soc. Am. J.* 32, 180–186.
- Haude, W., 1952. Verdunstungsmenge und Evaporationskraft eines Klimas. *Ber. Dt. Wetterdienst US-Zone* 42, 225–229.
- Hoy, A., Schucknecht, A., Sepp, M., Matschullat, J., 2014. Large-scale synoptic types and their impact on European precipitation. *Theor. Appl. Climatol.* 116, 19–35.
- Hseu, Z.-Y., Chen, Z.-S., 1996. Saturation, reduction, and redox morphology of seasonally flooded Alfisols in Taiwan. *Soil Sci. Soc. Am. J.* 60, 941–949.
- IPCC, 2014. *Climate Change 2014: Synthesis Report. Contribution of Working Groups I, II and III to the Fifth Assessment Report of the Intergovernmental Panel on Climate Change* [Core Writing Team, R.K. Pachauri and L.A. Meyer (eds.)]. IPCC, Geneva, Switzerland.
- IUSS Working Group WRB, 2015. *World reference base for soil resources 2014, update 2015*. FAO, Rome, Italy.
- Jenkinson, B.J., Franzmeier, D.P., 2006. Development and evaluation of iron-coated tubes that indicate reduction in soils. *Soil Sci. Soc. Am. J.* 70, 183–191.
- Mansfeldt, T., 2003. In situ long-term redox potential measurements in a dyked marsh soil. *J. Plant Nutr. Soil Sc.* 166, 210–219.
- Mansfeldt, T., 2004. Redox potential of bulk soil and soil solution concentration of nitrate, manganese, iron, and sulfate in two gleysols. *J. Plant Nutr. Soil Sc.* 167, 7–16.
- Mansfeldt, T., 2020. Soil redox potential. In: Wessel-Bothe, S., Weihermüller, L. (Eds.), *Field Measurement Methods in Soil Science*. Borntraeger Science Publishers, Stuttgart, Germany, pp. 19–41.
- Megonigal, J.P., Patrick, W.H., Faulkner, S.P., 1993. Wetland identification in seasonally flooded forest soils - soil morphology and redox dynamics. *Soil Sci. Soc. Am. J.* 57, 140–149.
- Mehra, O.P., Jackson, M.L., 1960. Iron oxide removal from soils and clays by a dithionite-citrate system buffered with sodium bicarbonate. *Clay Clay Miner.* 7, 317–327.
- Nakamura, K., Katou, H., Suzuki, K., Honma, T., 2018. Air-filled porosity as a key to reducing dissolved arsenic and cadmium concentrations in paddy soils. *J. Environ. Qual.* 47, 496–503.
- Orlowsky, B., Gerstengarbe, F.W., Werner, P.C., 2008. A resampling scheme for regional climate simulations and its performance compared to a dynamical RCM. *Theoret. Appl. Climatol.* 92, 209–223.
- Owens, P.R., Rutledge, E.M., Osier, S.C., Gross, M.A., 2001. The relationship of soils containing liquefaction features and redoximorphic features to perched seasonal water tables in the Lower Mississippi River Valley. *Quarter. Intern.* 78, 45–51.
- Potsdam Institute for Climate Impact Research, 2013. *STARS Klimaszenarien. Potsdam, Germany*.
- Pfeiffer, E.-M., Eschenbach, A., Munch, J.C., 2017. Boden. In: Brasseur, G.P., Jacob, D., Schuck-Zöller, S. (Eds.), *Klimawandel in Deutschland - Entwicklung, Folgen, Risiken und Perspektiven*. Springer, Heidelberg, pp. 203–213.
- Rabenhorst, M.C., Burch, S.N., 2006. Synthetic iron oxides as an indicator of reduction in soils (IRIS). *Soil Sci. Soc. Am. J.* 70, 1227–1236.
- Reddy, K.R., DeLaune, R.D., 2008. *Biogeochemistry of Wetlands - Science and Applications*. CRC Press, Boca Raton, FL, USA.
- Scheffer, F., Schachtschabel, P., 2018. *Lehrbuch der Bodenkunde*, 17th ed. Spektrum Akademischer Verlag, Heidelberg.
- Schindler, U., Durner, W., von Unold, G., Müller, L., 2010. Evaporation method for measuring unsaturated hydraulic properties of soils: extending the measurement range. *Soil Sci. Soc. Am. J.* 74, 1071–1083.
- Schwertmann, U., 1964. Differenzierung der Eisenoxide des Bodens durch Extraktion mit Ammoniumoxalat-Lösung (in German). *Z. Pflanzenernaehr. Dueng. Bodenkd.* 105, 194–202.
- Soil Survey Staff, 2014. *Keys to Soil Taxonomy. Twelfth Edition ed. USDA-Natural Resources Conservation Service, Washington, USA*.
- Tsubo, M., et al., 2007. Effects of soil clay content on water balance and productivity in rainfed lowland rice ecosystem in Northeast Thailand. *Plant Prod. Sci.* 10, 232–241.
- UMS, 2015. *Manual HYPROP, Munich, Germany*.
- Vepraskas, M.J., 2015. Redoximorphic Features for Identifying Aquic Conditions, Technical Bulletin 301. North Carolina State University, Raleigh, NC, USA.
- Vepraskas, M.J., Wilding, L.P., 1983. Aquic moisture regimes in soils with and without low chroma colors. *Soil Sci. Soc. Am. J.* 47, 280–285.
- Whitfield, M., 1974. Thermodynamic limitations on the use of the platinum electrode in E_H measurements. *Limnol. Oceanogr.* 19, 857–865.